Eur Biophys J (2010) 39:229–239
DOI 10.1007/s00249-009-0527-9

ORIGINAL PAPER

Molecular dynamics simulations reveal that AEDANS is an inert fluorescent probe for the study of membrane proteins

Werner L. Vos · Marieke Schor · Artur Baumgaertner · D. Peter Tieleman · Marcus A. Hemminga

Received: 14 May 2009 / Revised: 9 July 2009 / Accepted: 22 July 2009 / Published online: 11 August 2009

Abstract Computer simulations were carried out of a number of AEDANS-labeled single cysteine mutants of a small reference membrane protein, M13 major coat protein, covering 60% of its primary sequence. M13 major coat protein is a single membrane-spanning, α-helical membrane protein with a relatively large water-exposed region in the N-terminus. In 10-ns molecular dynamics simulations, we analyze the behavior of the AEDANS label and the native tryptophan, which were used as acceptor and donor in previous FRET experiments. The results indicate that AEDANS is a relatively inert environmental probe that can move unhindered through the lipid membrane when attached to a membrane protein.

Keywords Membrane proteins · Side-chain conformations · Tryptophan · Energy transfer (FRET) · Computer simulation

The more you see: spectroscopy in molecular biophysics.

W. L. Vos · M. Schor · M. A. Hemminga (✉)
Laboratory of Biophysics, Wageningen University, P.O. Box 8128, 6700 ET Wageningen, The Netherlands
e-mail: marcus.hemminga@wur.nl

A. Baumgaertner
Institut für Festkörperforschung, Forschungszentrum Jülich, Jülich, Germany

D. P. Tieleman
Department of Biological Sciences, University of Calgary, Calgary, Canada

M. A. Hemminga
Dreijenlaan 3, 6703 HA Wageningen, The Netherlands

Abbreviations

AEDANS	*N*-(acetylaminoethyl)-5-naphthylamine-1-sulfonic acid
FRET	Fluorescence (or Förster) resonance energy transfer
DOPC	1,2-Dioleoyl-*sn*-glycero-3-phosphocholine

Introduction

Fluorescence resonance energy transfer (FRET) is becoming increasingly popular as a tool to study membrane protein structure and to monitor conformational changes in membrane proteins (Corry et al. 2005; Gandi and Isacoff 2005; Máthyus et al. 2006). Unlike nuclear magnetic resonance (NMR) spectroscopy and X-ray crystallography, FRET cannot provide high-resolution structural information on membrane proteins. On the other hand, the technique has obvious advantages in that it is applicable over a wide range of experimental conditions and has superior sensitivity. However, to obtain distance constraints from FRET experiments, it is in general necessary to use fluorescent labels that are foreign to the protein. The use of probes introduces uncertainties in the interpretation of the FRET data, and in the extrapolation to the native structure of the protein. Clearly, to fully exploit FRET as a structural technique, it is vital that we understand the factors that govern the conformation and dynamics of fluorescent labels used in structural studies.

Only recently have fluorescent labels been taken into account explicitly in molecular modeling studies (Corry and Jayatilaka 2008; Gustiananda et al. 2004; Schröder et al. 2005; VanBeek et al. 2007). Similar approaches have

been carried out for the simulation of electron spin resonance (ESR) spectra of spin-labeled phospholipids (Håkansson et al. 2001) and proteins (DeSensi et al. 2008; Steinhoff et al. 2000). The fluorescent probe studies demonstrate that it is crucial to take into account the orientation, dynamics, and conformational space of the fluorescent labels for the calculation of accurate energy transfer efficiencies. For this reason, it is important to learn what factors affect the orientation and conformation of the fluorescent labels used in FRET experiments. This is especially true in the case of fluorescent labeled membrane proteins, where specific interactions of the fluorescent label with the phospholipid bilayer are an additional factor complicating the interpretation of fluorescence experiments. Moreover, due to the low dielectric environment inside the lipid bilayer, the effect of neighboring residues on the behavior of a fluorescent label could be more pronounced in the case of membrane proteins. Several molecular dynamics simulation studies have been performed to date that attempt to understand the relationship between the conformational behavior of a fluorescent label and the conformational features of a polymer on an atomic level (see, for instance, Kosovan et al. 2006 and VanBeek et al. 2007). Even though a number of modeling studies have taken fluorescent labels into account explicitly (Sparr et al. 2005), no systematic study on the behavior of fluorescent labels covalently attached to membrane proteins has been carried out to date.

Here, we perform molecular dynamics simulations of a number of AEDANS-labeled single cysteine mutants of a small reference membrane protein, M13 major coat protein, covering 60% of its primary sequence. M13 major coat protein is a single membrane-spanning, α-helical membrane protein with a relatively large water-exposed region in the N-terminus (Vos et al. 2009). We analyze the behavior of the AEDANS label and the native tryptophan, which were used as acceptor and donor in our previous FRET experiments (Nazarov et al. 2006, 2007; Vos et al. 2005, 2007b). The effect of lipids on the tryptophan and AEDANS conformational space is quantified and discussed. The effect of neighboring side-chains in a low-dielectric membrane environment is studied by comparison with simulations of a series of AEDANS-labeled polyalanine peptides. Our data show that the effect of both lipids and of neighboring side-chains on the AEDANS conformational space is limited. Thus AEDANS is an excellent fluorescent label to probe the direct chemical environment of membrane proteins, which is quite unhindered by neighboring amino acid side-chains, lipid or water molecules. As such, our approach could help to develop a general strategy to study membrane protein structure and function in the future using AEDANS as a probe in FRET or other fluorescence experiments.

Methodology

Details of the computer simulations

A straight α-helical conformation of M13 major coat protein, as proposed by Vos et al. (2005, 2009), was used as a starting conformation. The α-helix was constructed using the computer program Swiss PDBviewer (Guex and Peitsch 1997). The AEDANS label was incorporated into the molecular model in an extended configuration with all chain dihedral angles at 180° using the computer program MOLMOL (Koradi et al. 1996). Proteins were inserted into DOPC bilayers using the method of blowing up the bilayer on a grid and shrinking it again as described in Kandt et al. (2007). The proteins were positioned with a tilt angle of 23° relative to the bilayer normal, according to the orientation as determined in the literature with the valine residue at position 29 positioned at the center of the bilayer with its side-chain pointing downwards (Koehorst et al. 2004). Simulated systems contained the labeled protein, 126 DOPC molecules (63 per leaflet), and approximately 8,840 simple point charge (SPC) water molecules (Berendsen et al. 1981).

As a control for interactions between the protein side-chains and the AEDANS label, polyalanine helices (25 residues) with the labeled cysteine at various positions (2, 5, 10, 13, 17, 20, 23) were incorporated parallel to the z-axis in additional simulations with the same DOPC membrane. The rest of the parameters for the simulations of the polyalanine simulations were identical to the parameters used in the case of the coat protein.

For all mutants a 10-ns molecular dynamics simulation was performed after energy minimization and a short protein-restrained run. All simulations were performed with GROMACS 3.3.1 (Berendsen et al. 1995; Lindahl et al. 2001) and the optimized potential for liquid simulations (OPLS) all-atom protein force field (Tieleman et al. 2006) with the lipid parameters from Berger et al. (1997), combined with the SPC water model (Berendsen et al. 1981). The force field parameters for the AEDANS label were calculated using the Jaguar software (Schrödinger 2000) and can be obtained from the authors on request.

The temperature was set to 310 K for all simulations. Water, lipids, and protein were coupled separately to a Berendsen thermostat at 1 atm with a coupling constant of 0.1 ps (Berendsen et al. 1984). The pressure was coupled semi-isotropically to a Berendsen thermostat using a coupling constant of 1 ps and a compressibility of 4.5×10^{-5} atm^{-1} in the xy plane and normal to the membrane. A cutoff of 1.4 nm was used for van der Waals interactions. Long-range electrostatic interactions were calculated using the particle-mesh Ewald (PME) algorithm (Darden et al. 1993). The bonds were constrained with LINCS

(Hess et al. 1997), allowing for a 2-fs time step. To avoid biasing due to the starting configuration of the dihedral angles the first 2 ns of simulation time were discarded. The orientation factor κ^2 and energy transfer efficiency E were calculated for each frame of the remaining 8 ns of the trajectory and averaged. The rest of the analyses was performed with VMD (Humphrey et al. 1996).

Calculation of the energy transfer efficiency from the molecular dynamics simulations

The energy transfer efficiency is related to the distance between the donor and the acceptor and to the orientation of the two chromophores via (Dale and Eisinger 1976):

$$< E_i > = \left\langle \frac{\kappa_i^2}{C^{-1}R_i^6 + \kappa_i^2} \right\rangle. \quad (1)$$

For simplicity, neglecting effects of Boltzmann weighting, i runs over all possible conformations of the donor and the acceptor. Parameter E is the energy transfer efficiency, and κ^2 is the orientation factor as defined in Eq. 2. Parameter C describes the refractive index of the medium, the spectral overlap integral characteristic for this donor–acceptor pair, and the quantum yield of the donor in the absence of acceptors. This parameter is independent of the orientations of the donor and acceptor. It was determined to be 2.9×10^8 Å^6 in our previous work (Vos et al. 2005). The distance between the donor and the acceptor, R, is taken as the distance between the middle of the central bond of the indole and middle of the central bond of the dansyl chromophore.

The orientation factor κ^2 is related to the orientation of the donor transition dipole moment and acceptor absorption dipole moment (Gustiananda et al. 2004):

$$\kappa^2 = (\cos\theta_T - 3\cos\theta_D \cos\theta_A)^2. \quad (2)$$

Here, θ_T is the angle between the donor transition dipole moment and the acceptor absorption dipole moment, θ_D is the angle between the donor transition dipole moment and donor–acceptor interconnecting vector, and θ_A is the angle between the absorption dipole moment and the donor–acceptor interconnecting vector. The indole chromophore has two emitting states that are dependent on solvent polarity. In apolar solvents, the chromophore emits from the L_b state, whereas in polar solvents, the chromophore emits from the L_a state (Albinsson and Norden 1992; Sobolewski and Domcke 1999). Since in our case, tryptophan is buried inside the phospholipid membrane, being a hydrophobic environment, we will assume that the indole chromophore emits exclusively from the L_b state. Chemically, the tryptophan side-chain is very similar to 5-methylindole, having a carbon atom connected to the indole ring at the same position. Therefore, we expect the electronic configuration in tryptophan to be similar to that in 5-methylindole, enabling us to use the transition dipole moment of the L_b state of 5-methylindole as reported in the literature (Albinsson and Norden 1992) in our calculations of κ^2. This results in vector **D** shown in Fig. 1. The value and orientation of the absorption dipole moment of the AEDANS dansyl chromophore (vector **A** in Fig. 1) was taken from the literature, using the absorption dipole moment of 1,5-ACCys-AEDANS at 330 nm (Van der Heide et al. 1992). The calculation of the angles θ_T, θ_D, and θ_A as well as the calculation of the distance between the donor and acceptor was done using a PERL script.

Results

Depending on the initial configuration of a molecular dynamics simulation the phospholipid bilayer can take considerable time to equilibrate. For this reason we took a pre-equilibrated phospholipid bilayer as a starting configuration in all our simulations, and we used the INFLATEGRO script (Kandt et al. 2007) to insert the proteins, thereby minimizing disturbances of the lipids. To evaluate equilibration of the phospholipids, the area per lipid was analyzed over an extended simulation time of 30 ns (data not shown) for the AEDANS-labeled A18C and A27C mutant. During the first 2 ns of the simulation, the area per lipid decreased from $\sim$0.75 to $\sim$0.65 nm^2 for both mutants, in good agreement with values reported in the literature (Tieleman et al. 2006). This indicates that after $\sim$2 ns the bilayer is sufficiently equilibrated for our purpose of evaluating the behavior of the AEDANS probe and the tryptophan side-chain. Therefore, the rest of our analyses were performed over the timeframe 2–10 ns.

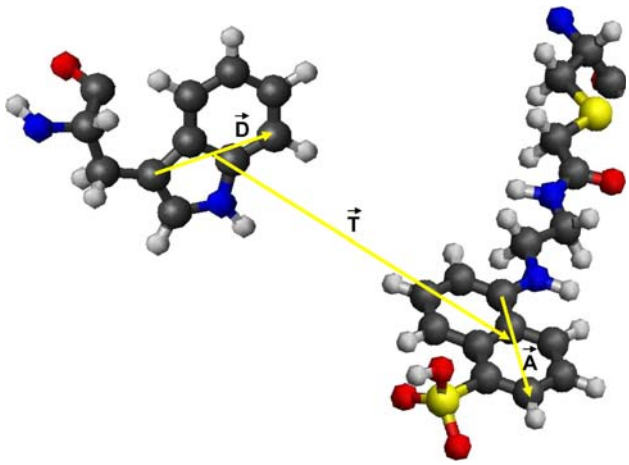

Fig. 1 Vectors of the tryptophan emission dipole (**D**), the AEDANS absorption dipole (**A**), and the interconnecting vector (**T**) used for the calculation of the orientation factor κ^2

Both the tryptophan side-chain and the AEDANS label adopt different conformations depending on the position of the AEDANS-labeled cysteine residue for membrane-embedded M13 coat protein mutants. This is illustrated in Fig. 2, which shows a surface plot of the tryptophan side-chain (blue) and the AEDANS label (red) over the course of the entire simulation for three representative AEDANS label positions: a mutant in the N-terminus (A16C), in the transmembrane segment (V29C), and in the C-terminus (S46C). In the case of the mutants A16C and S46C, the tryptophan surface plot appears more disc shaped, whereas the tryptophan surface plot for the V29C mutant is more spherical, indicative of different rotameric states during the course of the simulation. The AEDANS conformational space has a confined, disc-like shape in the case of the V29C mutant. Also for the A16C mutant, the AEDANS conformational space is relatively confined, whereas the conformational space of the S46C mutant has a bilobal shape, indicative of two major rotameric states.

During the simulations, membrane-embedded M13 coat protein remains close to an α-helix, enabling the use of the long axis of the helix as a reference to describe the orientation of the tryptophan and AEDANS side-chains. Thus, to quantify the conformational space occupied by the tryptophan side-chain, the angle of the tryptophan emission dipole moment with the long axis of the helix, ϕ_W, is depicted in Fig. 3 for membrane-embedded wild-type M13 coat protein and the mutants A16C, V29C, and S46C. In the case of the wild-type protein, the angular distribution of the tryptophan dipole moment with helical axis is symmetrical, centered on a value of 70°. The angular distributions of the mutants A16C and S46C are also symmetrical, centered on 65° and 70°, respectively. However, in the case of the V29C mutant, the angular distribution resembles two peaks, centered on values of 70° and 95°, respectively.

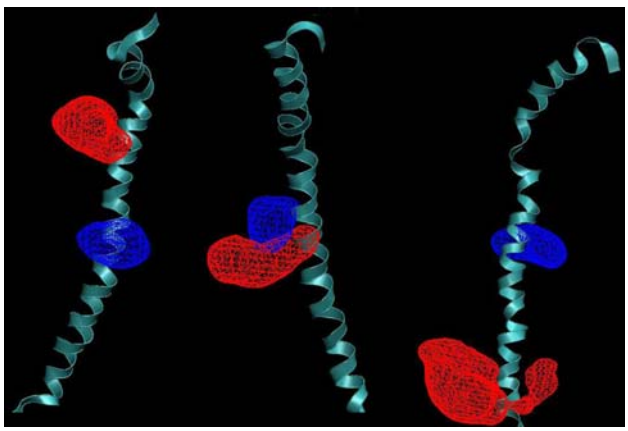

Fig. 2 Space-filling representation of the conformational space of the tryptophan side-chain (*blue*) and of the AEDANS-labeled cysteine residue (*red*) over the course of 8-ns simulation time for membrane-embedded AEDANS-labeled A16C, V29C, and S46C M13 coat protein mutants, respectively. The protein is represented as a *grey ribbon*

An overview of values of the center of the distributions describing the tryptophan conformational space for all mutants is given in Fig. 4. For most mutants one peak is observed centered at a value of ϕ_W around 60°. Some mutants show a second peak at a higher value of ϕ_W, mostly centered on 85°. An exception is observed for mutants A7C and A9C, where the value of ϕ_W of the second peak is 115° and 120°, respectively. Only in the case of mutant A18C are three peaks observed, giving a third value for ϕ_W of 118°. All values of ϕ_W fall within the range from 50° to 120°, indicating that the tryptophan emission dipole has a tendency to adopt a perpendicular orientation with respect to the helical axis. Throughout the AEDANS label position, no clear trend is observable in the values of ϕ_W. Furthermore, no large deviations from the value of the wild-type protein ($\phi_W = 70°$) are observed. These observations indicate that the effect of the AEDANS label on the tryptophan conformational space is limited.

In Fig. 5, the angle between the AEDANS absorption dipole and long axis of the protein helix, ϕ_A, is depicted for membrane-embedded M13 coat protein mutants A16C, V29C, and S46C. In the case of mutant A16C, the angular distribution of the AEDANS absorption dipole with respect to the helical axis is centered on a value of 80°. For mutant V29C, two peaks are observed in the angular distribution: one large peak centered on 50° and a smaller peak centered on 110°. The angular distribution of mutant S46C shows two peaks, centered at 20° and 65°.

In Fig. 6, the values of the center of the distributions describing the AEDANS conformational space are depicted. The values of ϕ_A fall within a range from 25° to 125°, indicating a wider distribution of conformational space of the AEDANS label as compared with the tryptophan side-chain, probably due to the longer AEDANS linker. Since the protein makes a tilt of 23° with respect to the membrane normal (Koehorst et al. 2004), the smallest values of ϕ_A imply that for certain mutants the AEDANS label is almost aligned with the lipid tails. Similar as in the case of tryptophan (Fig. 4), no clear trend can be observed in the values of ϕ_A, although it is obvious that the AEDANS conformational space varies strongly among different positions of the cysteine point mutation.

For the membrane-embedded M13 coat protein, the behavior of the AEDANS label is expected to be determined by three main factors: (1) the local rotations of the AEDANS side-chain attached to the protein backbone, (2) the restrictions of the rotamers by the backbone and side-chains of the neighboring amino acid residues, and (3) the restrictions imposed by the surrounding lipids.

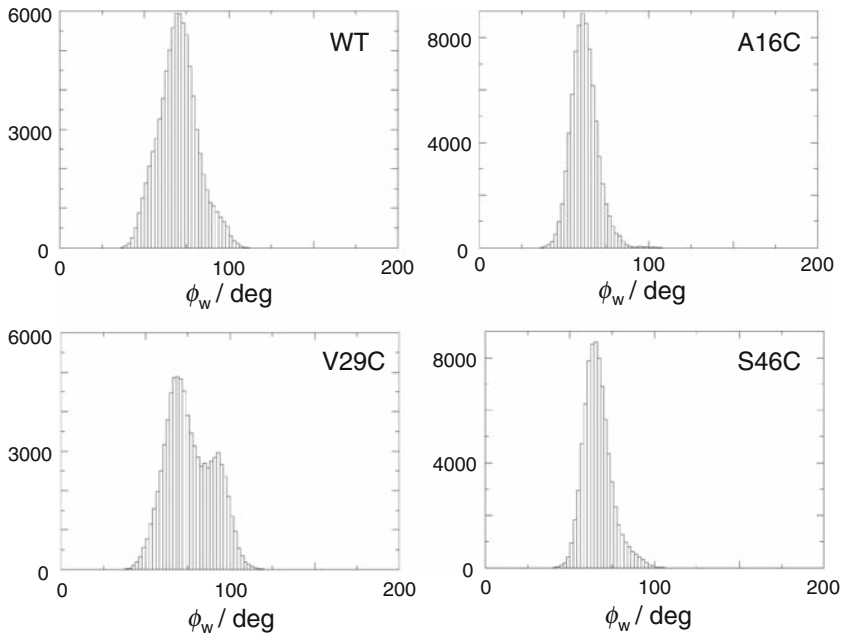

Fig. 3 Distribution of the angle between the tryptophan emission dipole moment and the helical axis for membrane-embedded wild-type M13 coat protein (WT), and the mutants A16C, V29C, and S46C

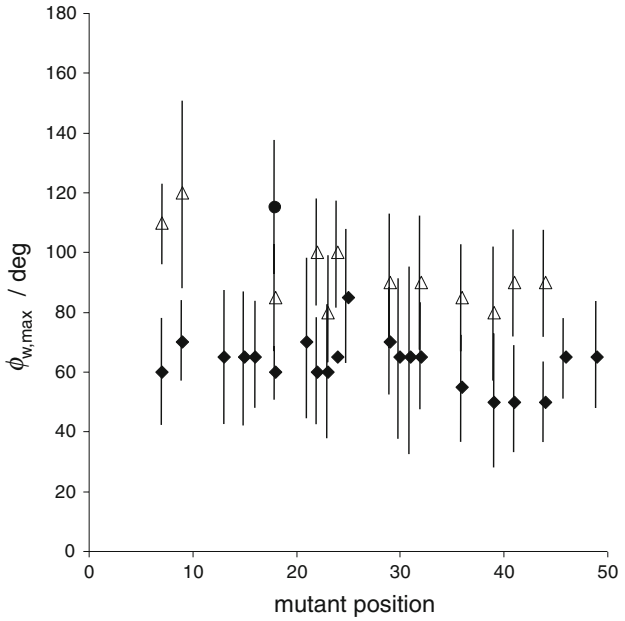

Fig. 4 Center of the distribution of angles between the tryptophan dipole and helical axis of the M13 coat protein, $\phi_{W,max}$, for all different mutants as a function of AEDANS label position. The *filled diamonds* represent the lowest values of the angles found. The *open triangles* represent the angles in case a second peak is observed. The *filled circle* represents the case of three peaks (mutant A18C). For well-resolved peaks, error margins were estimated based on the width of the peak at half height

To investigate these possibilities, an additional series of molecular dynamics simulations was carried out, using a 25-residue membrane-spanning α-helical polyalanine with a single AEDANS-labeled cysteine point mutation at different positions in the helix. Even though polyalanines do not form a transmembrane helix in vitro (Lewis et al. 2001), polyalanines are frequently used in molecular dynamics simulations as model transmembrane α-helices (Choma et al. 2001; Govaerts et al. 2001). Since the alanine side-chain is relatively small, specific interactions between the polyalanine helix and the AEDANS label are expected to be minimal, making it an ideal model transmembrane helix for our purpose. Therefore, in case of the polyalanine helix the conformational space of the AEDANS label is expected to be determined mainly by restrictions imposed by the surrounding lipids. The AEDANS conformational space varies strongly among different positions of the cysteine point mutation, as shown by the values of ϕ_A in Fig. 7. All values of ϕ_A fall within a range from 20° to 100°, indicating a slightly narrower distribution of conformational space of the AEDANS labels in polyalanine as compared with AEDANS labels attached to M13 coat protein (Fig. 6). This might be related to the more homogeneous structure of the polyalanine-membrane system.

Discussion

The goal of this work is to advance fluorescent techniques, in particular FRET, as tools to study membrane protein structure through studying the effect of the lipids and neighboring side-chains on the conformational space of a fluorescent labels attached to a model membrane protein.

To evaluate the implications of our findings with respect to the energy transfer efficiencies measured in our previous work (Vos et al. 2005), the energy transfer efficiencies

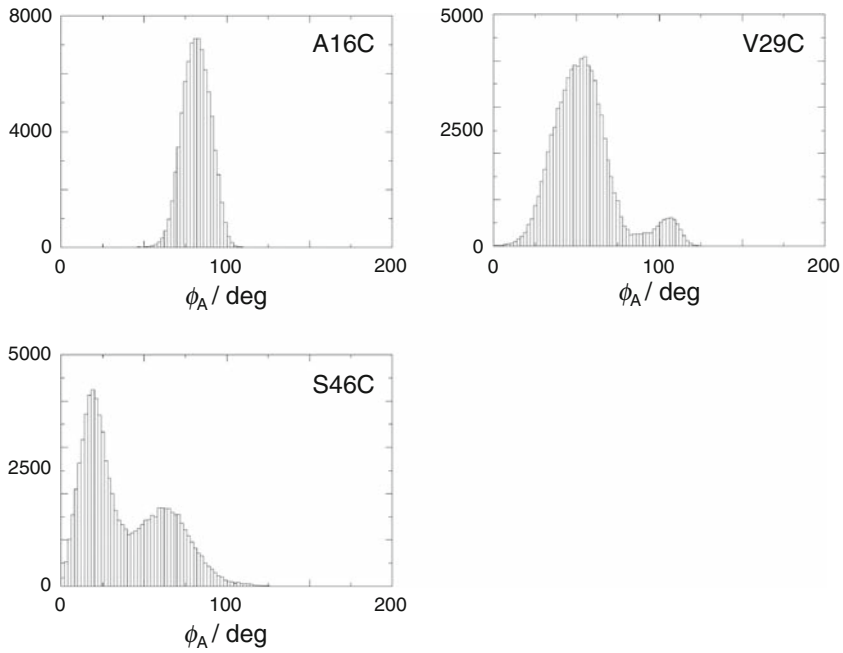

Fig. 5 Distribution of the angle between the AEDANS excitation dipole moment and the helical axis for membrane-embedded M13 coat protein mutants A16C, V29C, and S46C

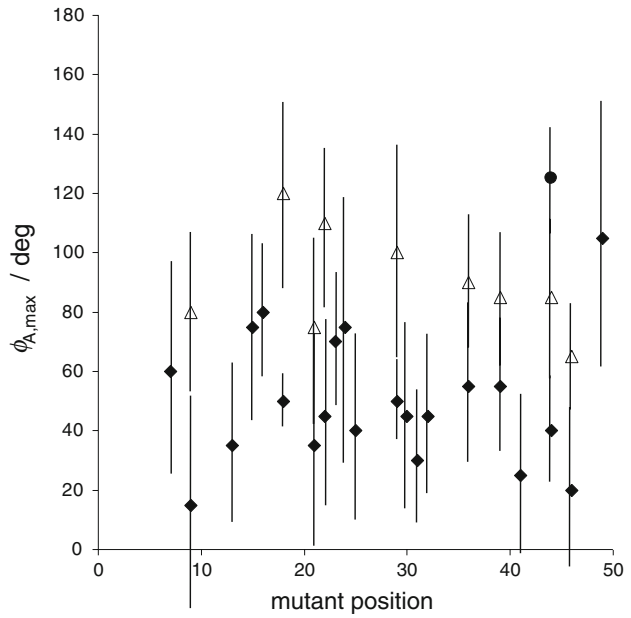

Fig. 6 Center of the distribution of the angles between the AEDANS absorption dipole and the helical axis of the M13 coat protein, $\phi_{A,max}$, for all different mutants as a function of AEDANS label position. The *filled diamonds* represent the lowest values of the angles found. The *open triangles* represent the angles in case a second peak is observed. The *filled circle* represents the case of three peaks (mutant 18). For well-resolved peaks, error margins were estimated based on the width of the peak at half height

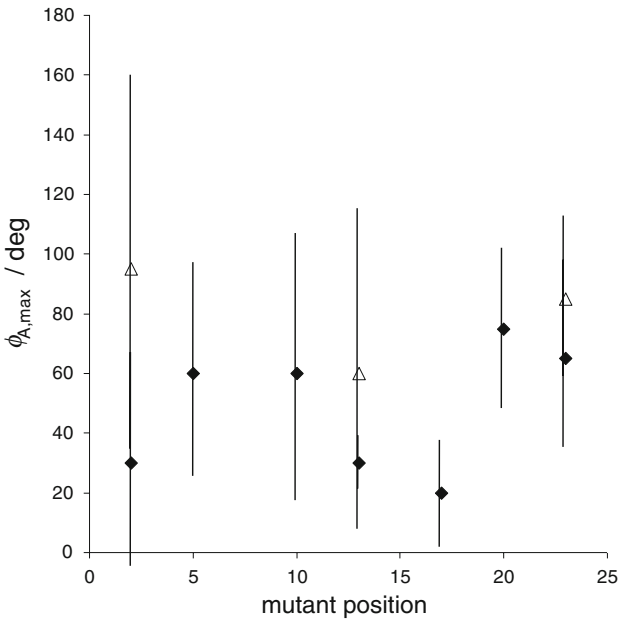

Fig. 7 Center of the distribution of the angles between the AEDANS absorption dipole and the helical axis, $\phi_{A,max}$, for all different mutants in the case of a membrane-embedded polyalanine helix. The *filled diamonds* represent the lowest values of the angles found. The *open triangles* represent the angles in case a second peak is observed. For well-resolved peaks, error margins were estimated based on the width of the peak at half height

calculated using Eq. 2 are depicted in Fig. 8. When the donor–acceptor pair in the experimental ensemble has the same fixed orientation or the same extent of dynamic averaging it is valid to substitute a single or average value for κ^2 in Eq. 2 (Dale and Eisinger 1979). Qualitatively, the energy transfer efficiencies calculated here are in good agreement with the experimental values for mutant positions 1–39, which could suggest that sampling might be sufficient, even though it is not complete for all individual mutants. However, the quality of the fit is not improved

much compared with the values calculated in our previous work based on the $<\kappa^2> = 0.67$ approximation. For mutant positions 40–50, the theoretical efficiencies appear systematically lower than the experimentally measured efficiencies. The main observation from the energy transfer efficiencies depicted in Fig. 8 is therefore that the energy transfer efficiencies in the C-terminus of the protein (mutants 40–50) show a systematic deviation towards lower values. Interestingly, recent FRET studies by our group on the same protein reconstituted in bilayers of hydrophobic mismatch indicate that residues 38–50 have a high propensity for helical deformation (Vos et al. 2007a). It is therefore likely that the discrepancy between the theoretical efficiencies calculated in the work presented here and the previously measured experimental efficiencies are due to the α-helical starting structure that was used in silico, whereas the helix would be more distorted in vitro. However, since the protein backbone is effectively rigid during the time span of the simulations, this will most likely not have an effect on the AEDANS or the tryptophan conformational space, which is the focus of the current work.

The surface plots in Fig. 2 of the tryptophan side-chain and of the AEDANS label of mutant V29C suggest a direct interaction between the tryptophan side-chain and the AEDANS label. The tryptophan and the AEDANS chromophores appear to be oriented in parallel planes, suggesting that the two chromophores are strongly interacting. The tryptophan conformation is best described as a disc-like conformation, which is also visible in the case of the A16C and S46C mutants. In this disc-like conformation,

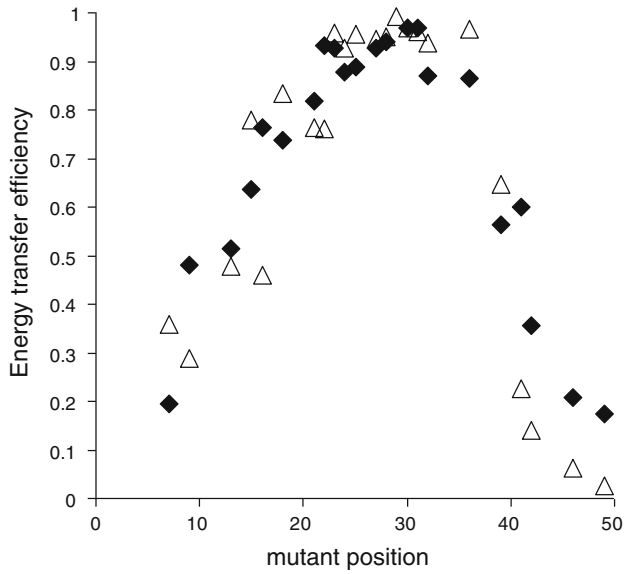

Fig. 8 Experimental (*filled diamonds*) and theoretical (*open triangles*) energy transfer efficiencies for the AEDANS-labeled mutants used in the molecular dynamics simulations

which is observed in the simulation of all mutants, the tryptophan emission dipole makes an angle of ~70° with the helical axis and the tryptophan emission and AEDANS absorption dipoles are more likely to align. Fig. 4 shows that this conformation of $\phi_W = 60°$ is present for most mutants. For a large number of mutants, a second conformation is observed, represented by a peak centered on a value $\phi_W = 90°$. A third conformation, with $\phi_W = 115°$, is visible in the case of the A7C and A9C mutants. The first conformation, with a value $\phi_W = 70°$, could be the conformation with the lowest energy. Therefore this conformation is present for most single cysteine mutant positions. The other two conformations are not always probed, although the second conformation, with a value $\phi_W = 90°$, shows up in ~50% of all mutants. The third conformation is the rarest, only showing up in 14% of all mutants. Only in the case of the A18C mutant are all three conformations present in a single simulation. The fact that there is no apparent correlation between the position of the AEDANS label and the conformational space of the tryptophan suggests that the differences between the different mutants and simulations are caused by incomplete probing of the tryptophan conformational space rather than by specific interactions affecting the energy of the different tryptophan rotameric states. Even though 10 ns of simulation time represents a considerable amount of computational time, such a simulation might not be sufficient for exhaustive probing of the tryptophan conformational space. To address this issue, the angle of tryptophan dipole with the local helix axis over the simulation time was evaluated for a selection of mutants: 7, 15, 23, 31, 36, 41, and 46 (data not shown). The main implications of this analysis are summarized in Table 1. Except for the mutant S46C, tryptophan shows many transitions between the different conformations, indicating that sampling is significant. The tryptophan conformational space is thus well described by three different rotameric states, even though not all conformational states appear in each simulation.

Compared with the tryptophan emission dipole moment, the values of the angular distribution of the AEDANS absorption dipole moment is wider. The maxima of the ϕ_A values cannot be categorized into groups with almost discrete values, possibly because the conformational space of the AEDANS group is much larger than that of the tryptophan side-chain due to the long linker between the AEDANS chromophore and the protein backbone. For comparison, the AEDANS group is linked to the protein backbone by seven bonds about which the chromophore can rotate freely, compared with two bonds with free rotation in the case of tryptophan, making the AEDANS conformational space significantly larger.

However, even though the values for the maxima of the AEDANS angular values do not fall into neatly defined

categories, it is worthwhile to analyze the angular distribution of the AEDANS dipole with the helical axis further. This is done by categorizing the values of the maxima depicted in Fig. 5 into different groups: groups A, B, C, D, E, and F, corresponding to values of ϕ_A of 10°–30°, 30°–50°, 50°–70°, 70°–90°, 90°–110°, and 110°–130°, respectively. The results of this analysis are depicted in Fig. 9 (white bars). Groups A, E, and F, representing the most extreme values of ϕ_A, are least densely populated. Possibly, this reflects a purely statistical effect, indicating that AEDANS behaves like a relatively unperturbed vector, sweeping a conical surface. Throughout all the molecular dynamics simulations, ϕ_A ranges from 30° to 50° (group B). Even though the values of ϕ_A throughout the different simulations do not form a peak themselves, the results presented here do suggest that values $30° \leq \phi_A \leq 90°$ (groups B, C, and D) have a higher probability, regardless of the mutant position, and that extreme ϕ_A values have a lower probability. To evaluate whether sampling of the AEDANS conformational space is significant, the angle of the AEDANS dipole with the local helix axis over the simulation time was evaluated for a selection of mutants: 7, 15, 23, 31, 36, 41, and 46 (data not shown). The conclusions of this analysis are summarized in Table 1. Mutants 15 and 46 show only a few transitions, indicating that sampling is limited, while for the other mutants the angles sample a significant range with many transitions, indicating that sampling is significant in most cases.

To elucidate to what extent specific interactions with the side-chains or with the neighboring lipid and water molecules affect the AEDANS conformational space, an additional set of simulations of AEDANS-labeled polyalanine was analyzed in the same way. The angular distribution diagrams for both the AEDANS-labeled coat protein and the AEDANS-labeled polyalanine show a considerable spread, depending on the position of the mutation. Since specific interactions between the AEDANS label and the amino acid side-chains are not very important in the case of the polyalanine helix, the spread in the maxima of the angular distribution functions which is observed in the simulations of AEDANS-labeled polyalanine is not caused by specific, position-dependent interactions with neighboring side-chains. This raises the question of what determines the spread in ϕ_A values observed in Fig. 7, i.e., whether specific interactions between the label and lipid and water molecules are responsible or whether the different simulations probe different parts of the AEDANS conformational space, which is, in fact, very similar for the various mutant positions.

If the interactions between the label and the lipids change the AEDANS conformational space, a certain degree of symmetry would be expected in Fig. 7. For instance, the distance between the mutant positions 2 and 5 and the lipid head group region is roughly the same as the distance between mutant positions 23 and 20 and the opposite lipid head group region. This implies that the AEDANS groups are exposed to approximately the same lipid environment for mutants 2 and 5 as for mutants 23 and 20, respectively. However, the ϕ_A values for positions 2 and 23 are different, as are the ϕ_A values for positions 5 and 20. Also for the other mutant positions, where the AEDANS label is buried deeper into the bilayer, no symmetry can be inferred from the ϕ_A values. Therefore, it is not likely that the interaction with the lipid and water molecules is the decisive factor that determines the spread in ϕ_A values as observed in the polyalanine simulations. More likely, the spread in ϕ_A values observed here is

Table 1 Sampling analysis of the angles of the tryptophan and AEDANS dipoles with the local helix axis over the simulation time (10 ns) for the AEDANS-labeled coat protein. The analysis was carried out for a selection of mutants

Mutant position	Tryptophan	AEDANS
7	20°–160°, many transitions[a]	0°–180°, many transitions
15	20°–160°, many transitions	0°–180°, few transitions
23	0°–180°, many transitions	20°–150°, many transitions
31	10°–180°, many transitions	50°–120°, many transitions
36	0°–180°, many transitions	0°–160°, many transitions
41	20°–120°, many transitions	50°–120°, many transitions
46	Few transitions[b]	Few transitions

[a] About 100 transitions per ns

[b] About 1 transition per ns

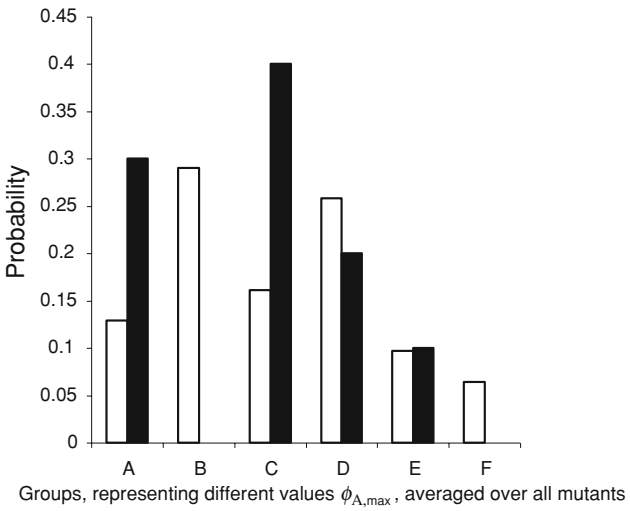

Fig. 9 Probability of finding the AEDANS labels in various conformations averaged over all mutants for AEDANS-labeled polyalanine (*black bars*) and for AEDANS-labeled coat protein (*white bars*). Groups A, B, C, D, E, and F, correspond to values of $\phi_{A,max}$ of 10°–30°, 30°–50°, 50°–70°, 70°–90°, 90°–110°, and 110°–130°, respectively

caused by the fact that different simulations probe different parts of the AEDANS conformational space, as is the case even for the much smaller tryptophan side-chain. In fact, in the case of AEDANS, the spread in ϕ_A values is expected to be even bigger than the spread in ϕ_W values in the case of the tryptophan side-chain, due to the larger mass of the AEDANS label and the increased magnitude of the AEDANS conformational space.

The comparison between the ϕ_A values in the case of AEDANS-labeled coat protein and AEDANS-labeled polyalanine indicates that specific interactions between the AEDANS label and neighboring side-chains do not have a large effect on the AEDANS conformational space. Secondly, the fact that the distribution in ϕ_A values in the case of the AEDANS-labeled polyalanine is essentially random suggests that the position spread in the AEDANS conformational space is not strongly affected by interactions with neighboring lipid and water molecules. More likely, the spread in ϕ_A values between the different mutant positions is caused by incomplete probing of the conformational space in each individual simulation.

To test the latter idea, it is worthwhile to make a comparison between the distribution of the ϕ_A values in the case of the AEDANS-labeled coat protein and the AEDANS-labeled polyalanine, averaged over all mutants. If position-dependent specific interactions between the label and neighboring side-chains, and between the label and surrounding lipid and water molecules, do not have a large effect on the AEDANS conformational space, the conformational space as observed in the simulations of the polyalanine simulations would be similar to the conformational space as observed in the simulations of the coat protein simulations across all different mutants. The ϕ_A values found across the different simulations of M13 coat protein and polyalanine are depicted in Fig. 9 (white bars for coat protein, black bars for polyalanine). Clearly there are differences between the behavior of AEDANS when attached to a polyalanine helix and to M13 major coat protein. For instance, when attached to a polyalanine single helix the label is not found in group B, whereas the label is frequently present in group B when it is attached to coat protein. Possibly, this difference is because the number of mutants for the polyalanine is only limited as compared with those for coat protein, which means that sampling is less exhaustive for the label attached to the polyalanine helix then for the label attached to coat protein. To illustrate this, we compare combined probabilities for groups A and B, C and D, and E and F, respectively, for the AEDANS-labeled polyalanine and AEDANS-labeled coat protein. The combined probabilities for A/B, C/D, and E/F are 0.3, 0.6, and 0.1 in the case of polyalanine. For coat protein, the combined probabilities are 0.4, 0.4, and 0.2. Hence, for both the AEDANS-labeled polyalanine helix and the coat and for the AEDANS-labeled coat protein, the label is most likely to be found in groups C/D, although in the case of AEDANS-labeled polyalanine the label is equally likely to be found in groups A/B. For both AEDANS-labeled polyalanine and coat protein, the label is least likely to be found in groups E/F.

This result suggests that the average conformational space for AEDANS is similar in the case of the polyalanine simulations as in the case of the M13 simulations, indicating that specific interactions between the label and neighboring side-chains do not affect the AEDANS conformational space significantly. In summary, our results indicate that neither specific interactions between the AEDANS label and the lipid or water molecules, nor interactions between the AEDANS label and neighboring side-chains, have a large effect on the AEDANS conformational space. Interestingly, this finding advocates the use of AEDANS as a relatively inert environmental probe that can move relatively unhindered through the lipid membrane.

An important factor when using FRET as a spectroscopic tool is the mutual orientation of the donor and acceptor during energy transfer. For this reason, we evaluate the average value of the orientation factor for all different AEDANS-labeled major coat protein mutants over the course of the simulation, $<\kappa^2>$, depicted in Fig. 10. We note that this value represents a static average, and therefore the extrapolation to energy transfer efficiencies as measured in a fluorescence experiment is not straightforward. However, for our purpose of evaluating potential systematic trends in the mutual orientation of donor and acceptor dipoles, evaluation of $<\kappa^2>$ suffices. For most mutants, the value of $<\kappa^2>$ is lower than 0.67 (the isotropic dynamic average that is frequently used to calculate distances from energy transfer experiments). In

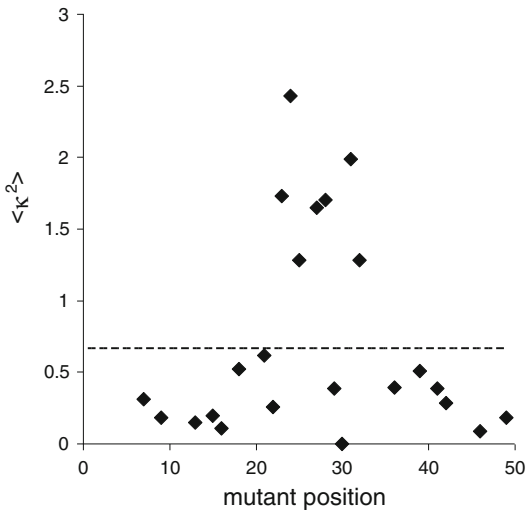

Fig. 10 Implications for the average orientation factor $<\kappa^2>$

certain cases, $<\kappa^2>$ is almost zero, indicating a perpendicular orientation between the tryptophan emission dipole and the AEDANS absorption dipole. Notably, for mutant positions 23–32, $<\kappa^2>$ is strongly increased to as high as 2.5, approaching the theoretical maximum of 4, indicating that the dipoles are almost aligned. For this reason it is worthwhile to evaluate the average value of the orientation factor κ^2 for all different AEDANS-labeled major coat protein mutants over the course of the simulation, $<\kappa^2>$, as depicted in Fig. 10. For most mutants, the value $<\kappa^2>$ is lower than 2/3, which is the isotropic dynamic average that is frequently used to calculate distances from energy transfer experiments. In certain cases, $<\kappa^2>$ is almost zero, indicating a perpendicular orientation between the tryptophan emission dipole and the AEDANS absorption dipole. Notably, for mutant positions 23–32, the energy transfer for most mutants is strongly increased to as high as 2.5, approaching the theoretical maximum of 4, indicating that the tryptophan emission dipole and the AEDANS absorption dipole are almost aligned, at least through part of the simulation.

Even though the effect of neighboring side-chains on the AEDANS and tryptophan conformational space is limited, the data presented in Fig. 9 suggest that there is some interaction between the AEDANS and the tryptophan group, resulting in an increased $<\kappa^2>$ value for mutants in the transmembrane region. This could suggest a small degree of stacking between the AEDANS and tryptophan chromophores, as illustrated in Fig. 2, increasing the probability of dipole alignment. On the other hand, Fig. 6 gives no indications of a systematic effect on the overall conformational space, suggesting that the increase in $<\kappa^2>$ could be due to an indirect effect, with both tryptophan and AEDANS aligning along the lipid acyl chains.

Concluding remarks

Our computer simulations suggest that the conformational space of the AEDANS label is only slightly affected by the presence of amino acid side-chains or lipids. This finding advocates the use of AEDANS as a relatively inert environmental probe that is structurally unhindered by the membrane lipids. As such, AEDANS fluorescence spectroscopy and FRET could contribute to the development of a general strategy to study membrane protein structure and function in the future.

Acknowledgments This work was partially supported by a travel grant provided to W.L.V. from The Netherlands Organization for Scientific Research (NWO). We thank Drs. Christian Kandt, Luca Monticelli, and Zhitao Xu for their assistance with the topology building and setting up of the molecular dynamics simulations. D.P.T. is an Alberta Heritage Foundation for Medical Research Senior Scholar and Canadian Institutes for Health Research New Investigator. Work in D.P.T.s group is supported by CIHR.

References

Albinsson B, Norden B (1992) Excited-state properties of the indole chromophore: electronic transition moment directions from linear dichroism measurements: effect of methyl and methoxy substituents. J Phys Chem 96:6204–6212

Berendsen HJC, Postma JPM, WFv Gunsteren, Hermans J (1981) Interaction models for water in relation to protein hydration. In: Pullman B (ed) Intermolecular forces. Reidel, Dordrecht, pp 331–342

Berendsen HJC, Postma JPM, Van Gunsteren WF, DiNola A, Haak JR (1984) Molecular dynamics with coupling to an external bath. J Chem Phys 81:3684–3690

Berendsen HJC, van der Spoel D, van Drunen R (1995) GROMACS: a message-passing parallel molecular dynamics implementation. Comput Phys Commun 91:43–56

Berger O, Edholm O, Jähnig F (1997) Molecular dynamics simulations of a fluid bilayer of dipalmitoylphosphatidylcholine at full hydration, constant pressure, and constant temperature. Biophys J 72:2002–2013

Choma CT, Tieleman DP, Cregut D, Serrano L, Berendsen HJC (2001) Towards the design and computational characterization of a membrane protein. J Mol Graph Model 20:219–234

Corry B, Jayatilaka D (2008) Simulation of structure, orientation, and energy transfer between AlexaFluor molecules attached to MscL. Biophys J 95:2711–2721

Corry B, Rigby P, Liu Z-W, Martinac B (2005) Conformational changes involved in MscL channel gating measured using FRET spectroscopy. Biophys J 89:L49–L51

Dale RE, Eisinger J (1976) Intramolecular energy transfer and molecular conformation. Proc Natl Acad Sci USA 73:271–273

Dale RE, Eisinger J (1979) The orientational freedom of molecular probes. The orientation factor in intramolecular energy transfer. Biophys J 26:161–194

Darden T, York D, Pedersen L (1993) Particle mesh Ewald: An $N\cdot\log(N)$ method for Ewald sums in large systems. J Chem Phys 98:10089–10092

DeSensi SC, Rangel DP, Beth AH, Lybrand TP, Hustedt EJ (2008) Simulation of nitroxide electron paramagnetic resonance spectra from Brownian trajectories and molecular dynamics simulations. Biophys J 94:3798–3809

Gandi CS, Isacoff EY (2005) Shedding light on membrane proteins. Trends Neurosci 28:472–479

Govaerts C, Blanpain C, Deupi X, Ballet S, Ballesteros JA, Wodak SJ, Vassart G, Pardo L, Parmentier M (2001) The TXP motif in the second transmembrane helix of CCR5. J Biol Chem 16:13217–13225

Guex N, Peitsch MC (1997) SWISS-MODEL and the Swiss-PdbViewer: an environment for comparative protein modeling. Electrophoresis 18:2714–2723

Gustiananda M, Liggins JR, Cummins PL, Gready JE (2004) Conformation of prion protein repeat peptides probed by FRET measurements and molecular dynamics simulations. Biophys J 86:2467–2483

Håkansson P, Westlund PO, Lindahl E, Edholm O (2001) A direct simulation of EPR slow-motion spectra of spin labelled

phospholipids in liquid crystalline bilayers based on a molecular dynamics simulation of the lipid dynamics. Phys Chem Chem Phys 3:5311–5319

Hess B, Bekker H, Berendsen HJC, Fraaije JGEM (1997) LINCS: a linear constraint solver for molecular simulations. J Comput Chem 18:1463–1472

Humphrey W, Dalke A, Schulten K (1996) VMD: visual molecular dynamics. J Mol Graph 14:27–28

Kandt C, Ash WL, Tieleman DP (2007) Setting up and running molecular dynamics simulations of membrane proteins. Methods 41:475–488

Koehorst RBM, Spruijt RB, Vergeldt FJ, Hemminga MA (2004) Lipid bilayer topology of the transmembrane α-helix of M13 major coat protein and bilayer polarity profile by site-directed fluorescence spectroscopy. Biophys J 87:1445–1455

Koradi R, Billeter M, Wüthrich K (1996) MOLMOL: a program for display and analysis of macromolecular structures. J Mol Graph 14:51–55

Kosovan P, Limpouchova Z, Prochazka K (2006) Molecular dynamics simulation of time-resolved fluorescence anisotropy decays from labelled polyelectrolyte chains. Macromolecules 39:3458–3465

Lewis RNAH, Zhang Y-P, Hodges RS, Subczynski WK, Kusumi A, Flach CR, Mendelsohn R, McElhaney RN (2001) A polyalanine-based peptide cannot form a stable transmembrane α-helix in fully hydrated phospholipid bilayers. Biochemistry 40:12103–12111

Lindahl E, Hess B, van der Spoel D (2001) GROMACS 3.0: a package for molecular simulation and trajectory analysis. J Mol Model 7:306–317

Máthyus L, Szöllosi J, Jenei A (2006) Steady-state fluorescence quenching applications for studying protein structure and dynamics. J Photochem Photobiol B 83:223–236

Nazarov PV, Koehorst RBM, Vos WL, Apanasovich VV, Hemminga MA (2006) FRET study of membrane proteins: simulation-based fitting for analysis of membrane protein embedment and association. Biophys J 91:454–466

Nazarov PV, Koehorst RBM, Vos WL, Apanasovich VV, Hemminga MA (2007) FRET study of membrane proteins: determination of the tilt and orientation of the N-terminal domain of M13 major coat protein. Biophys J 92:1296–1305

Schröder GF, Alexiev U, Grubmüller H (2005) Simulation of fluorescence anisotropy experiments: probing protein dynamics. Biophys J 89:3757–3770

Schrödinger I (2000) JAGUAR 4.1. Schrödinger, Portland

Sobolewski AL, Domcke W (1999) Ab initio investigations on the photophysics of indole. Chem Phys Lett 315:293–298

Sparr E, Ash WL, Nazarov PV, Rijkers DTS, Hemminga MA, Tieleman DP, Killian JA (2005) Self-association of transmembrane α-helices in model membranes: importance of helix orientation and role of hydrophobic mismatch. J Biol Chem 280:39324–39331

Steinhoff H-J, Müller M, Beier C, Pfeiffer M (2000) Molecular dynamics simulation and EPR spectroscopy of nitroxide side chains in bacteriorhodopsin. J Mol Liq 84:17–27

Tieleman DP, MacCallum JL, Ash WL, Kandt C, Xu Z, Monticelli L (2006) Membrane protein simulations with a united-atom lipid and all-atom protein model: lipid–protein interactions, side chain transfer free energies and model proteins. J Phys Condens Matter 18:S1221–S1234

Van der Heide UA, Orbons B, Gerritsen HC, Levine YK (1992) The orientation of transition moments of dye molecules used in fluorescence studies of muscle systems. Eur Biophys J 21:263–272

VanBeek DB, Zwier MC, Shorb JM, Krueger BP (2007) Fretting about FRET: correlation between κ and R. Biophys J 92:4168–4178

Vos WL, Koehorst RBM, Spruijt RB, Hemminga MA (2005) Membrane-bound conformation of M13 major coat protein: a structure validation through FRET-derived constraints. J Biol Chem 280:38522–38527

Vos WL, Schor M, Nazarov PV, Koehorst RBM, Spruijt RB, Hemminga MA (2007a) Structure of membrane-embedded M13 major coat protein is insensitive to hydrophobic stress. Biophys J 93:3541–3547

Vos WL, Vermeer LS, Hemminga MA (2007b) Conformation of a peptide encompassing the proton translocation channel of vacuolar H^+-ATPase. Biophys J 92:138–146

Vos WL, Nazarov PV, Koehorst RBM, Spruijt RB, Hemminga MA (2009) From 'I' to 'L' and back again: the odyssey of membrane-bound M13 protein. Trends Biochem Sci 34:249–255